Research Journal of Applied Sciences, Engineering and Technology 9(4): 288-295, 2015
DOI:10.19026/rjaset.9.1407
ISSN: 2040-7459; e-ISSN: 2040-7467

Submitted: August 13, 2014 Accepted: October 12, 2014 Published: February 05, 2015

Research Article

Transformer Winding Deformation Profile using Modified Electrical Equivalent Circuit

M. Arul Sathya and S. Usa
Division of High Voltage Engineering, College of Engineering Guindy, Anna University,
Chennai- 600 025, Tamil Nadu, India

Abstract: This study presents a generalized methodology to predict the transformer winding deformation profile through Sweep Frequency Response Analysis using Finite Element Method based Magneto Structural Analysis and proposed modified equivalent circuit. Monitoring and diagnosis of fault in any power apparatus is necessary to increase the quality life of the apparatus. In general all the power transformers are designed to withstand the mechanical forces due to short circuit faults. However, mechanical forces may exceed the specified limits during severe incidents leading to winding deformation. Winding deformation is one of the causes for the power transformer outages. In the present work, deformation profile of the winding for different short circuit currents are computed using Finite Element Method based Magneto-structural analysis. The change in circuit parameters of the deformed windings are computed using Finite Element Method based field analyses and the corresponding Sweep Frequency Responses are obtained using the modified electrical equivalent circuit. From the change in resonance frequencies, the displacement profile of the winding can be predicted which will be useful for design engineers to check the withstand capability of transformer.

Keywords: Finite element method, RLC parameters, sweep frequency response analysis, transformer winding deformation

INTRODUCTION

In general, the magnitude of the fault currents depends upon the short circuit reactance of the test transformer (Waters, 1966). These currents cause high leakage flux which can be resolved into radial flux and axial flux resulting in axial and radial forces respectively. Depending on the distribution of forces and mechanical integrity of the windings the weakest region undergoes winding deformation. These forces not only displace/deform the windings but also affect the other transformer components such as clamping ring, flitch plates and frames. Geometrical changes in the windings cause deviations in its resonance frequencies indicating the positional or electrical variations of the internal components (Kraetge *et al*., 2009). Sweep Frequency Response Analysis (SFRA) is a powerful method for the detection and diagnosis of defects in the active part of power transformer which can deliver valuable information about the mechanical as well as the electrical changes in the windings parameters.

Kulkarni and Kumbhar (2007) have computed the force distribution due to short-circuit current in a split-winding transformers using Finite Element Analysis (FEA). Faiz *et al*. (2008) have analyzed the radial and axial electromechanical forces developed by the inrush and short circuit currents using 2D and 3D Finite Element Method (FEM) models. Ahn *et al*. (2012) have compared the simulated and measured forces in windings.

Zhang *et al*. (2014) have compared the frequency responses of both undeformed and radially deformed winding. Wang *et al*. (2010) have investigated the relationship between the winding deformation and the Vibration Sweep Frequency Response (VSFR) for 220kV transformer. Hashemnia *et al*. (2012) have simulated the frequency response signature for various mechanical faults such as axial displacement, buckling stress, disc space variation and bushing fault.

In the present study, deformation profile of the winding for different short circuit currents are computed using Magneto-structural analysis. The change in circuit parameters of the deformed windings are computed using Finite Element Method (FEM) based field analyses and the corresponding Sweep Frequency Responses (SFR) are obtained using the proposed modified electrical equivalent circuit. The above mentioned methodology will be useful for the design engineers in analyzing the force, displacement profiles, the resulting shift in resonant frequency and the change in impedances.

Corresponding Author: M. Arul Sathya, Division of High Voltage Engineering, College of Engineering Guindy, Anna University, Chennai- 600 025, Tamil Nadu, India

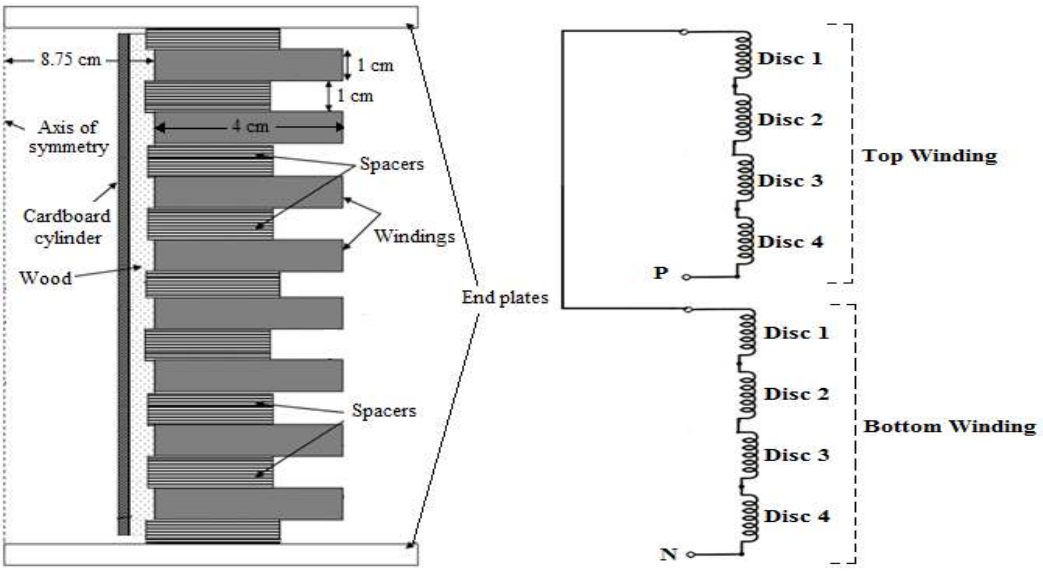

Fig. 1a: Details of the test transformer

Fig. 1b: Windings connection

MATERIALS

Winding under study: The transformer under study has two identical windings with 4 discs per winding as shown in Fig. 1a. Each disc has 10 turns. The windings are connected in such a way to simulate a transformer with the winding currents in the opposite directions (Fig. 1b).

METHODS

Displacement profile using magneto structural analysis: The electromagnetic force distribution and displacements in the windings are computed using FEM based Magneto-structural analysis. To check the computational methodology, short circuit test as per IEC Standard 60076-5 was conducted on similar windings with two discs per winding at On Load Gears, Ambattur, Chennai (Sathya *et al*., 2013) and the simulation results were validated with experimental displacements. Hence, the methodology is extended for 4 discs per winding (Fig. 1) for different currents.

Both the windings are energized equally for different short circuit currents in the opposite directions and the corresponding axial displacements along the length of the windings are computed using Magneto-structural analysis. It is observed that the displacements of the discs are not uniform and the geometrical representation of the windings with displaced disc positions for different current densities is given in Fig. 2.

Circuit parameters of displaced windings: In general, the transformer winding are modeled using R (resistance), L (inductance), C (capacitance) ladder network. FEM based Electromagnetic field solvers are used to extract the C (inter-turn (C_t) and inter-disc (C_d) capacitance and stray capacitance (C_g), L (self and mutual inductance) and R (resistance) of the winding. Figure 3 shows the details of the top/bottom winding.

Winding capacitance: The series capacitance of the winding is composed of two parts, inter-turn capacitances (C_t) and inter-disc capacitances (C_d). For axial deformation of transformer winding, the inter-turn capacitance remains the same whereas the inter disc capacitances changes as the distance between the discs vary. The capacitances are obtained by solving FEM based Electrostatic solver. Based on the displacements due to different currents, inter-disc capacitance for different gaps from 0.0033-0.03 m is computed (Fig. 4). The inter-turn capacitance of one disc is found to be 10.58 pF. Stray/shunt capacitance (C_g) is also calculated using Electrostatic solver.

Winding inductance: For axial deformation of the transformer winding, the self inductance of the winding remains same and the mutual inductance between the windings change with the displacement.

The total inductance of the winding is computed from total magnetic energy. In the case of multi-turns and/or multi-disc windings, there will be two inductive components namely self and mutual inductance between two sections. If the mutual inductance between the discs is L_{12}, the magnetic linkages λ_1 and λ_2 will be:

$$\lambda_1 = L_{11} I_1 + L_{12} I_2 \quad (1)$$

$$\lambda_2 = L_{22} I_2 + L_{21} I_1 \quad (2)$$

With L_1, L_2 the self inductance of the discs of 1 and 2 respectively and ($L_{21} = L_{12} = M$) the mutual inductance between the discs. The total magnetic energy is:

$$W_m = \frac{1}{2} [L_1 I_1^2 + 2 L_{12} I_1 I_2 + L_2 I_2^2] \quad (3)$$

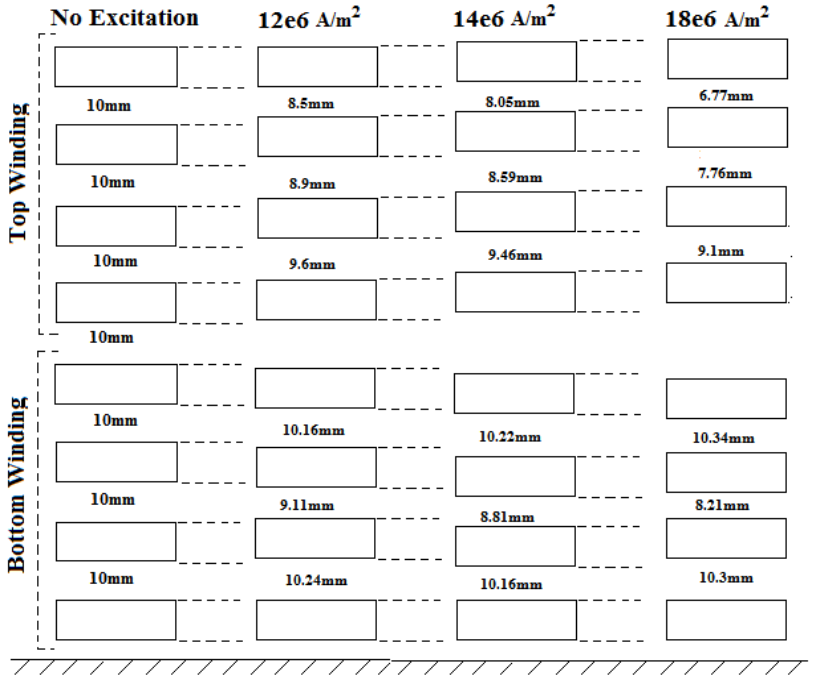

Fig. 2: Geometrical representation of the deformed windings for different current densities

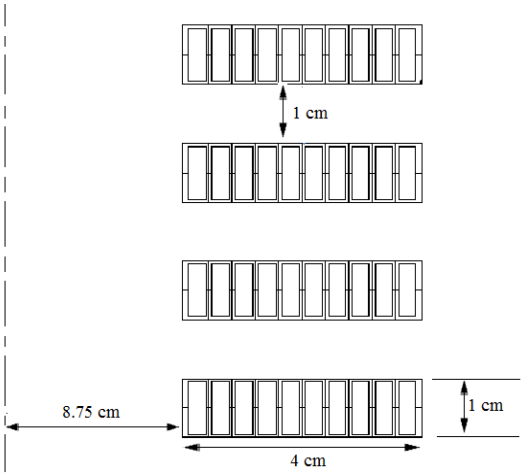

Fig. 3: Transformer winding

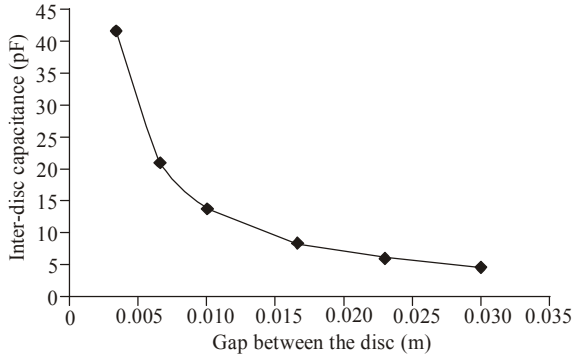

Fig. 4: Inter-disc capacitance for different inter disc distances

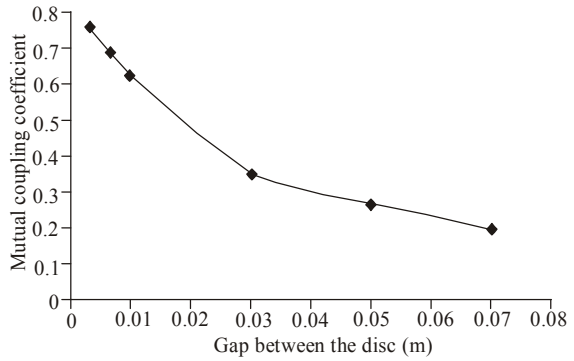

Fig. 5: Inductive coupling factor for different inter disc distances

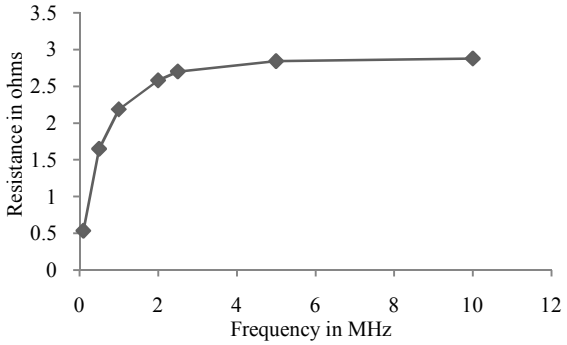

Fig. 6: Variation of winding resistance with frequency

In this case, since $I_1 = I_2$ and $L_1 = L_2$, the mutual inductance is:

$$L_{12} = \frac{W_m}{I^2} - L \quad (4)$$

and the mutual coupling coefficient (k_{12}) is:

$$k_{12} = \frac{L_{12}}{\sqrt{L_1 L_2}} \quad (5)$$

Magneto static solver is used to extract the inductances. The self-inductance of a disc is found to be 32.27μH. The change in the mutual coupling coefficient between the discs for different gaps is shown graphically in Fig. 5.

Winding resistance: The change in winding resistance with frequency due to skin effect is carried out by solving FEM based Eddy Current Solver and is shown in Fig. 6.

By using these equivalent circuit parameters, the SFRA are carried out.

RESULTS

Modified electrical equivalent circuit: Electrical equivalent circuit of transformer winding is represented by a combination of winding resistance, self-inductance, mutual inductance, inter-turn capacitance, inter-disc capacitance and stray capacitance. The basic electrical equivalent circuit of a transformer winding is shown in Fig. 7. The SFR for the unexcited winding is obtained using circuit simulation package and shown in Fig. 8.

In the above equivalent circuit, the inter-turn and inter-disc capacitances are represented as single capacitance (C_s). Due to axial deformation, there will be a change in inter disc capacitance which can be appropriately incorporated by separating the series winding capacitances (C_s) into inter turn (C_t) and inter-disc capacitance (C_d) and the varying inductive

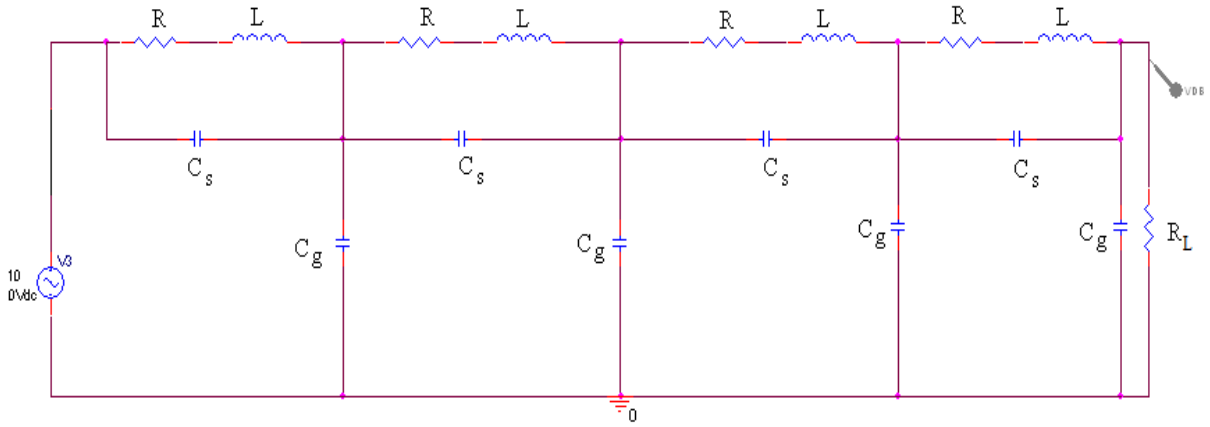

Fig. 7: Electrical equivalent circuit (basic circuit) of the winding

Table 1: Percentage change in resonance frequencies

Resonant frequency in (MHz)	Electrical equivalent circuit model (simulated)			% Error between simulated models and measured	
	Basic	Modified	Measured	Basic	Modified
f_{r1}	2.730	2.696	2.697	-1.2	0.04
f_{r2}	4.035	4.417	4.325	6.7	-2.13

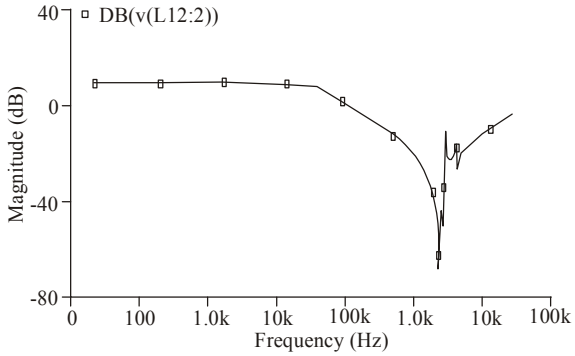

Fig. 8: Sweep frequency response of the unexcited winding (using basic circuit)

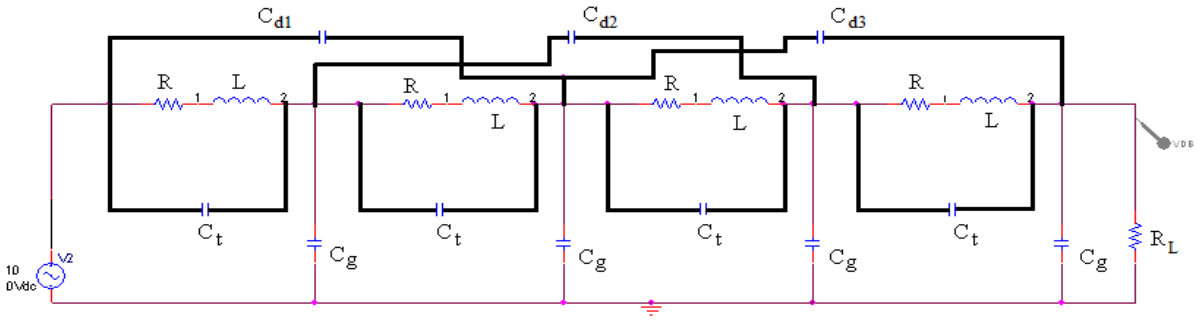

Fig. 9: Modified electrical equivalent circuit of the winding

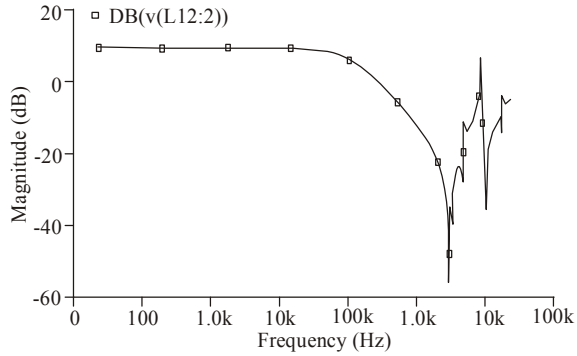

Fig. 10: Sweep frequency response of the unexcited winding with modified circuit

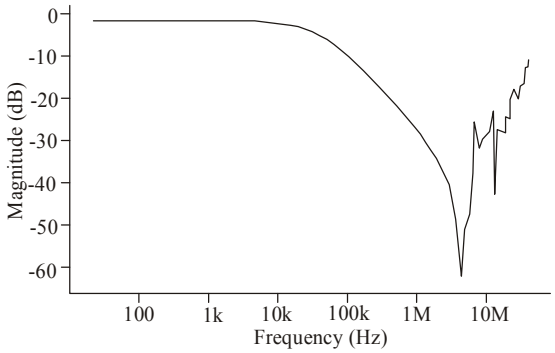

Fig. 11: Sweep frequency response of the unexcited winding (Measured)

coupling (k) between the discs are also incorporated. Figure 9 shows the proposed 'modified electrical equivalent circuit' with separated C_t and C_d. and the corresponding frequency response is shown in Fig. 10.

The SRF of the winding is also measured using a Sweep Frequency Response Analyzer (FRAX 101, Megger make) and is shown in Fig. 11.

From Fig. 8, 10 and 11, it is observed that SFR is improved with modified circuit (Table 1) and hence the modified circuit is considered for the further analyses.

DISCUSSION

SFRs for deformed windings: The proposed modified electrical equivalent circuit can model both axially and radially deformed winding by appropriately considering the changes in C_d, k and C_t, L respectively. In the present study, the windings are deformed only in axial direction due to radial force. For the displacements of discs reported in Section 3 for different currents, the corresponding C_d and k (Fig. 4 and 5) are incorporated appropriately in the proposed modified electrical equivalent circuit and the corresponding SFRs are computed. Figure 12a shows the computed SFRs of the top winding.

The windings are manually displaced and SFRs are measured for both the windings using SFR and Fig. 12b shows the measured SFRs of the top winding for different currents. It is observed from Fig. 12a and b,

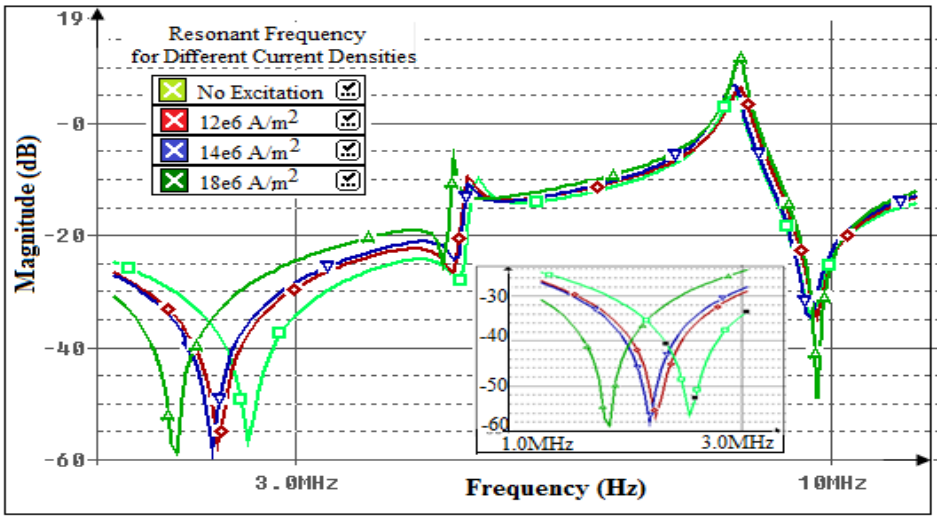

Fig. 12a: SFRs of the top winding for different currents (simulated)

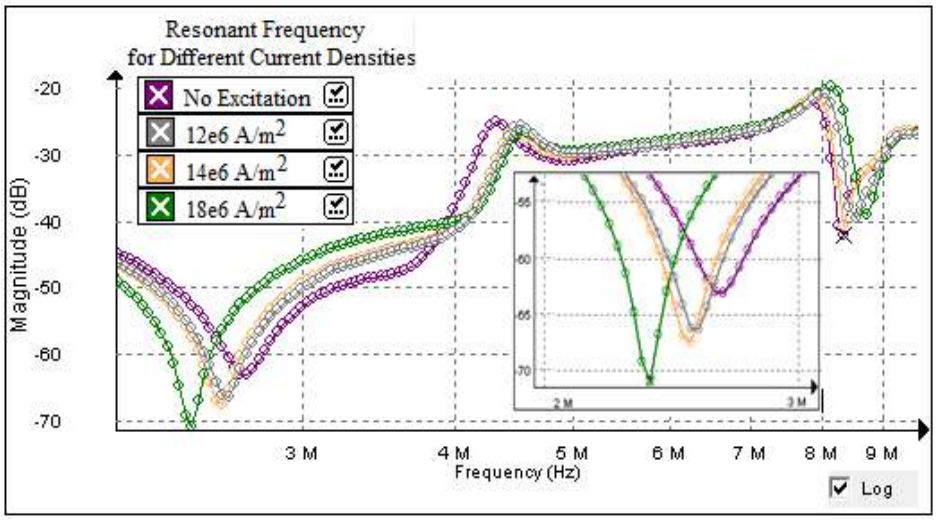

Fig. 12b: SFRs of the top winding for different currents (measured)

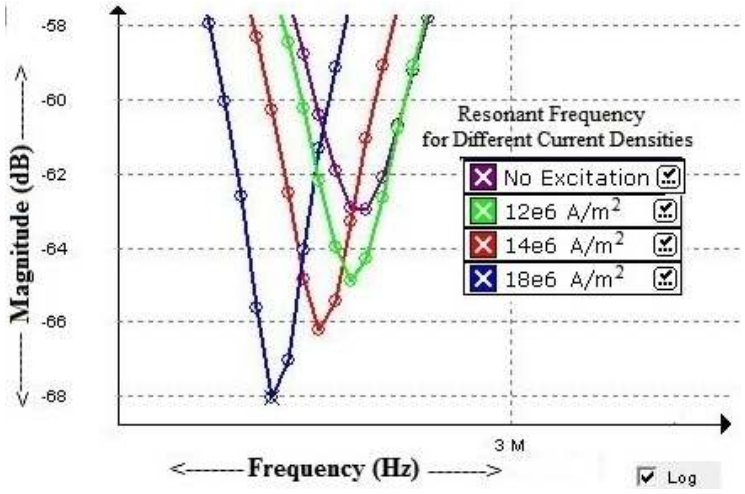

Fig. 13a: Shift in f_{r1} of bottom winding (measured)

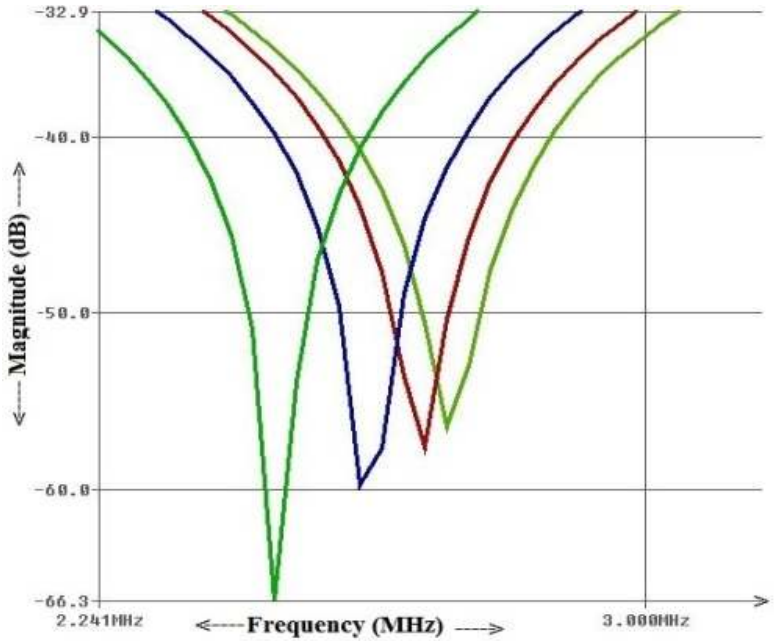

Fig. 13b: Shift in f_{r1} of bottom winding (simulated)

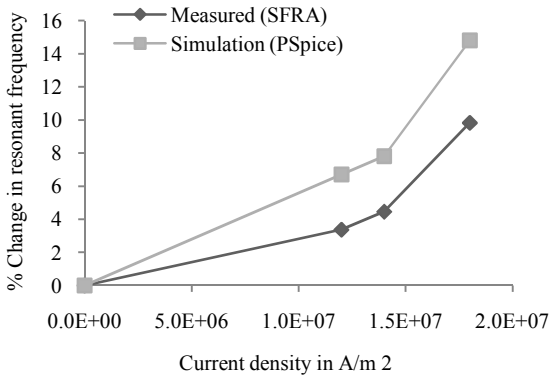

Fig. 14a: Percentage shift in fr1 for top winding

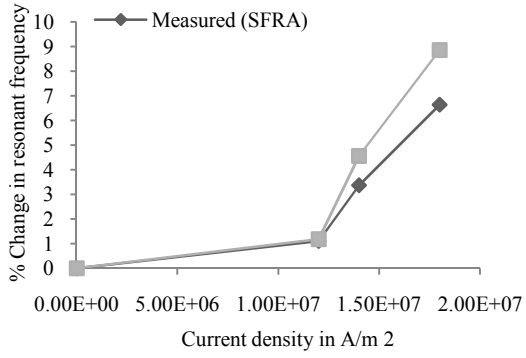

Fig. 14b: Percentage shift in fr1 for bottom winding

the varied displacements between the windings are modeled effectively using the proposed modified circuit with less than 4% error. It is also observed that the shift in first resonant frequency is predominant (Fig. 12a and b) and hence only the first resonant frequency is considered for forthcoming analyses.

Similarly the measured and simulated f_{r1} of bottom winding are shown in Fig. 13a and b respectively.

It is observed that the fr1 reduces with increasing currents and the same trend is observed in both measured and simulated SFRs for both the windings. For different short circuit currents, the percentage change in f_{r1} for top and bottom windings are given in Fig. 14a and b, respectively.

When the SFR of a deformed winding is obtained, the shift in the f_{r1} can be calculated with the help of the unexcited SFR signature from which the magnitude of the excitation current and the corresponding winding deformation profile can be predicted from Fig. 14. The above analysis can also be used to predict the withstand capability of transformer by calculating the winding impedance from the deformed winding dimensions at the design stage itself as per IEC Standard 60076-5.

CONCLUSION

The displacement of the transformer windings are computed using Finite Element Method based Magneto-structural analysis for different short circuit currents. The corresponding shift in resonance frequencies are predicted using the proposed modified electrical equivalent circuit and compared with measurement. The discussed approach will be useful for the design engineers in estimating the force, displacement profiles, change in SFRs and also the change in impedances for any short circuit currents at the design stage itself.

REFERENCES

Ahn, H.M., Y.H. Oh, J.K. Kim and J.S. Song, 2012. Experimental verification and finite element analysis of short-circuit electromagnetic force for dry-type transformer. IEEE T. Magn., 48(2): 819-822.

Faiz, J., B.M. Ebrahimi and T. Noori, 2008. Three- and two-dimensional finite-element computation of inrush current and short-circuit electromagnetic forces on windings of a three-phase core-type power transformer. IEEE T. Magn., 44(5): 590-597.

Hashemnia, N., A. Abu-Siada, M.A.S. Masoum and S.M. Islam, 2012. Characterization of transformer FRA signature under various winding faults. Proceeding of International Conference on Conditioning Monitoring and Diagnosis (CMD, 2012), pp: 446-449.

Kraetge, A., M. Kruger, J.L. Velasquez, H. Viljoen and A. Dierks, 2009. Aspects of the practical application of Sweep Frequency Response Analysis (SFRA) on power transformers. Proceeding of 6th Southern Africal Regional Conference (CIGRE, 2009).

Kulkarni, S.V. and G.B. Kumbhar, 2007. Analysis of short-circuit performance of split-winding transformer using coupled field-circuit approach. IEEE T. Power Deliver., 22(2): 936-943.

Sathya, M.A., A.J. Thomas and S. Usa, 2013. Prediction of transformer winding displacement from frequency response characteristics. Proceeding of IEEE 1st International Conference on Condition Assessment Techniques in Electrical Systems (CATCON), pp: 303-307.

Wang, F.H., J. Xu, Z.J. Jin and S.S. Gui, 2010. Experimental research of vibration sweep frequency response analysis to detect the winding deformation of power transformer. Proceeding of IEEE PES Transmission and Distribution Conference and Exposition, pp: 1-6.

Waters, M., 1966. The Short-circuit Strength of Power Transformer. McDonald & Co. Ltd., London.

Zhang, Z.W., W.H. Tang, T.Y. Ji and Q.H. Wu, 2014. Finite-element modeling for analysis of radial deformations within transformer windings. IEEE T. Power Deliver., 29(5): 2297-2305.